A Deuteron NMR Study on the Dynamics of Fluorobenzene Molecules Adsorbed on Graphite and Boron Nitride

B. Boddenberg and V. Grundke

Lehrstuhl für Physikalische Chemie II, Universität Dortmund, Dortmund, FRG

Z. Naturforsch. **46a**, 211–220 (1991); received November 2, 1990

The present ^{2}H NMR study gives some evidence that a film of fluorobenzene of about one monolayer thickness on graphite undergoes a 2D phase transition from a fluid like into a rotationally disordered solid phase at ca. 160–130 K, and subsequently a 2D solid-solid transition into an ordered phase at a temperature about 90 K. A multilayer film ($\theta = 8$) decomposes below about 200 K into a 3D bulk solid phase and an adsorbed film, of presumably monolayer thickness. It is concluded that the monolayer film spreads uniformly on the available surface with flat orientation of the molecules. These detailed statements can be obtained because the combined action of the intramolecular quadrupole interaction and the extramolecular magnetic shielding type coupling allows to relate the Z-axes of coordinate frames fixed in the support and fixed in the adsorbed molecule.

I. Introduction

In recent studies [1–5] it was demonstrated that deuteron (^{2}H) solid-state NMR spectroscopy can favourable be used to determine the orientation of molecules adsorbed on the basal planes of graphite from the characteristic asymmetries of the quadrupole patterns. These shape asymmetries are due to the circumstance that besides the electric quadrupole coupling the deuterons of the adsorbed molecules are acted on by the Zeeman field via a magnetic shielding tensor which has its origin in the solid support. It was found further [2, 6] that the shape asymmetries disappear if the deuteron-carrying molecules are no longer in close contact with the surface, e.g. if a microcrystalline bulk solid (3D) phase is formed in the void space left by the loosely packed adsorbent particles. This property can be used to study the separation of multilayer films at temperatures below the bulk triple point into 2D and 3D phases in equilibrium with each other.

The molecules studied so far exhibit either zero (benzene, p-xylene, mesitylene, mellitene) or small (toluene) electric dipole moments. At one monolayer surface coverage and, at least at low temperatures, these molecules are adsorbed flat on the graphite surface. This may be not so for molecules which exhibit a considerable dipole moment since in such cases the dipole-dipole forces are conceivable to prevent the flat orientation in the monolayer coverage regime and to lead to a non-wetting behaviour. The present study addresses these questions with fluorobenzene ($\mu = 1.60$ D [7]) adsorbed on graphite and, for comparison purposes, on hexagonal boron nitride.

Reprint requests to Prof. Dr. B. Boddenberg, Physikalische Chemie II, FB Chemie, Universität Dortmund, Otto-Hahn-Str. 6, D-4600 Dortmund 50.

II. Experimental

The adsorbents used for the present investigation were graphitized carbon black Graphon (Cabot Corp., Boston, Mass., USA) and microcrystalline hexagonal boron nitride (325 mesh, Alfa-Ventron, Danvers, Mass., USA) which have nitrogen BET specific surface areas of 80 and 15 m^2/g, respectively [1]. The adsorbent particles of both Graphon and boron nitride expose predominantly the (0001) crystal basal planes. Graphon consists of spherules of mean diameter of about 40 nm [8] agglomerated to chainlike structures which are bounded by stacks of graphite microcrystallites with linear dimensions of several nm both parallel and normal to the surface. Boron nitride, on the other hand, consists of terraced platelets with mean diameter of about 3 μm and diameter to thickness ratio of about 10 [1]. In contrast to Graphon the boron nitride powder exhibits a broad distribution of the particle sizes ranging from platelet diameters of about 100 nm to 10 μm.

The adsorbents were put into 10 mm outer diameter NMR glass-tubes, evacuated at slowly rising

0932-0784 / 91 / 0300-0211 $ 01.30/0. – Please order a reprint rather than making your own copy.

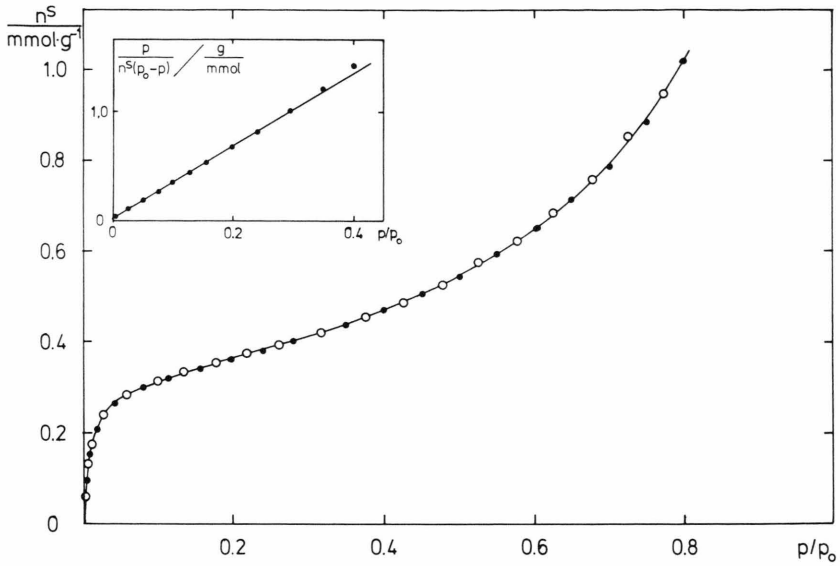

Fig. 1. Ad- and desorption isotherms of fluorobenzene on Graphon, 20 °C. (•) Adsorption; (○) desorption. The insert shows the BET-plot.

temperature, and finally baked at 450 °C under high vacuum ($p \lesssim 10^{-4}$ Pa) for about 12 hrs. Subsequently, calibrated amounts of fluorobenzene-d_5 (Sigma, St. Louis, USA) were chilled onto the samples to yield the surface coverages θ required. For fluorobenzene on Graphon the monolayer capacity ($n_m = 316$ μmol/g) was evaluated from the gravimetrically determined adsorption isotherm shown in Fig. 1 using the BET procedure of analysis. The fluorobenzene molecule cross section deduced from n_m and the nitrogen BET surface area cited before is $\omega = 0.42$ nm^2 which value is in close agreement with literature data for non-graphitic adsorbents [9]. Therefore, the definition of θ will be based on this value for each of the adsorbents used.

The NMR measurements were performed with the aid of a high power FT-NMR spectrometer (CXP 100, Bruker-Physik, Karlsruhe, Germany), operating at constant frequency 52.72 MHz, in conjunction with a nominal 8.1 T cryogenic magnet system (Oxford Instruments, Oxford, England). The ^{2}H spectra were obtained by Fourier-transformation of the free induction decays and/or of the quadrupole echoes (QE) generated with the pulse sequence $(\pi/2)_x - \tau - (\pi/2)_y - \tau$ [10]. Quadrature detection was always employed. In cases where spectra of widths larger than about 150 kHz showed up, the pulse flip angles were reduced to $(\pi/3)$ corresponding to pulse widths of about 3 μs. If not stated otherwise, the pulse delay time was set to a value in the range 30 to 50 μs.

III. Results

Figure 2a shows the deuteron NMR spectra of a monolayer of fluorobenzene-d_5 on Graphon at several selected temperatures between 240 and 75 K. The sequence of spectra may be subdivided into three temperature intervals in which well characterized spectrum shapes are exhibited: nearly Lorentzian type singlets of increasing width at half height $\delta\nu$ (240–160 K), powder patterns with prominent edge splitting $\Delta\nu$ of about 70 kHz and distinct shape asymmetry (130–110 K), and patterns of edge splitting 140 kHz (around 75 K). At temperatures between them, superpositions of the spectrum types of the respective neighbouring intervals show up. At the slightly lower coverage $\theta = 0.85$, the sequence of spectra is similar, but the corresponding lineshapes appear at about 10 K lower temperatures (Figure 2b).

The temperature dependence of the width at half height ($\delta\nu$) of the singlet lines of Fig. 2a and b is shown in Figure 3. In the Arrhenius type representation chosen straight lines are obtained over an extended temperature range. The activation energies evaluated from the slopes are 21 and 34 kJ mol^{-1} for the samples with coverages $\theta = 0.85$ and 1.0, respectively.

Figure 4 shows the temperature dependence (298 to 75 K) of the ^{2}H NMR spectra of C_6D_5F on boron nitride at surface coverage $\theta = 0.85$. Basically, the development of the width and shape of the spectra with temperature resembles that which is observed for

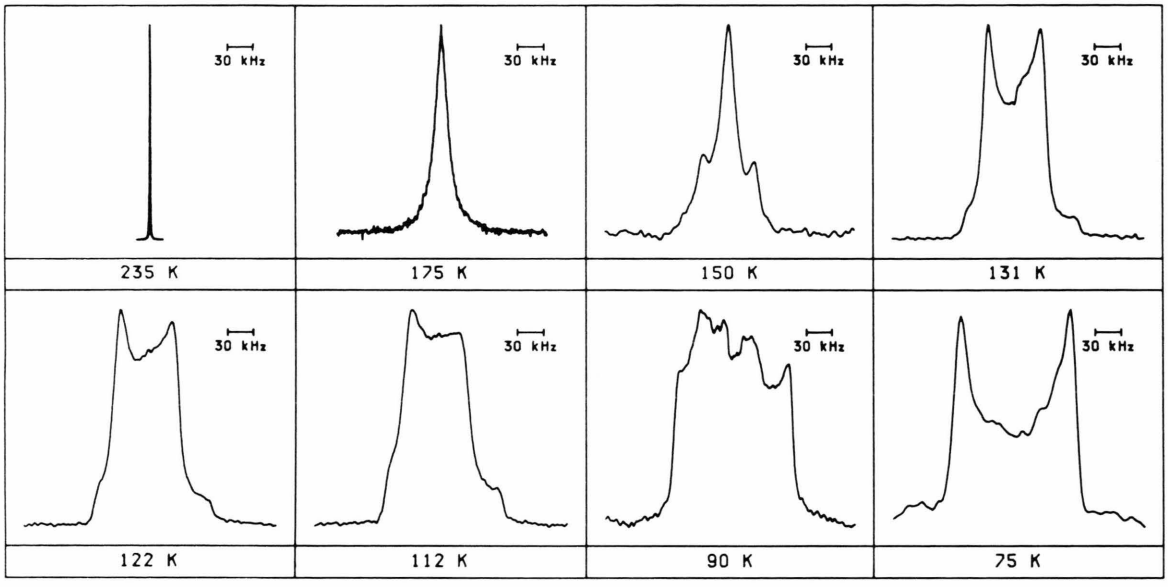

a

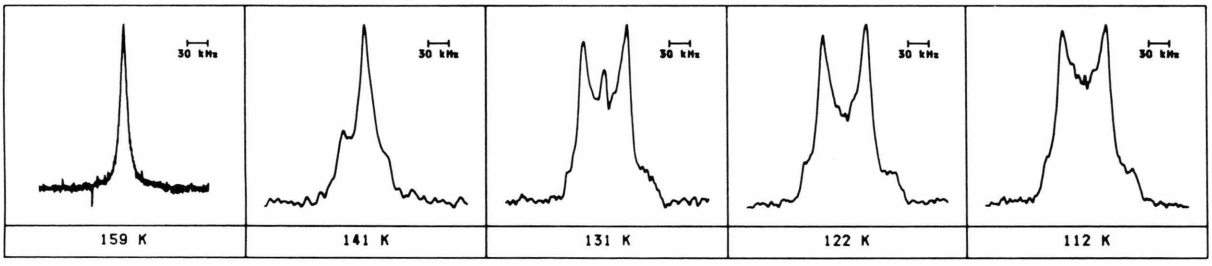

b

Fig. 2. ^{2}H NMR spectra of fluorobenzene adsorbed on Graphon. a) Surface coverage $\theta = 1.0$. b) Surface coverage $\theta = 0.85$. In all cases the frequency axis runs from right to left.

Graphon as the support. The comparison with Fig. 2a and b reveals, however, two major differences: (i) The quadrupole patterns with $\Delta\nu = 70$ kHz edge splitting (168 to 131 K) have their main and side edges symmetrically displaced with respect to the center frequency, and (ii) the singlets are considerably broader at a given temperature and their transformation into the quadrupole pattern type takes place at a higher temperature. At 159 K, for instance, the solid state pattern is fully developed with boron nitride, whereas the singlet shape is observed for Graphon (Fig. 2b) as the support.

Figure 5 shows the ^{2}H NMR spectra of C_6D_5F on Graphon, surface coverage $\theta = 8$, at several selected temperatures between 291 and 90 K. In contrast to the one monolayer sample (Fig. 2a), a $\Delta\nu = 140$ kHz Pake type pattern develops below about 200 K and is dominant at 169 K (the central singlet component ($\delta\nu \approx 10$ kHz), which was detected in the FID (not shown), is missing in the quadrupole-echo derived spectrum due to relaxation effects). At 131 K the spectrum obtained with a recycle delay time of 1 s consists of superimposed patterns of 70 and 140 kHz edge splittings. Performing the experiment with 0.1 s delay time saturates the broad component and leaves a 70 kHz asymmetric pattern of the same type as is observed for the one monolayer sample (Figure 2a). A similar behaviour is observed at 122 K.

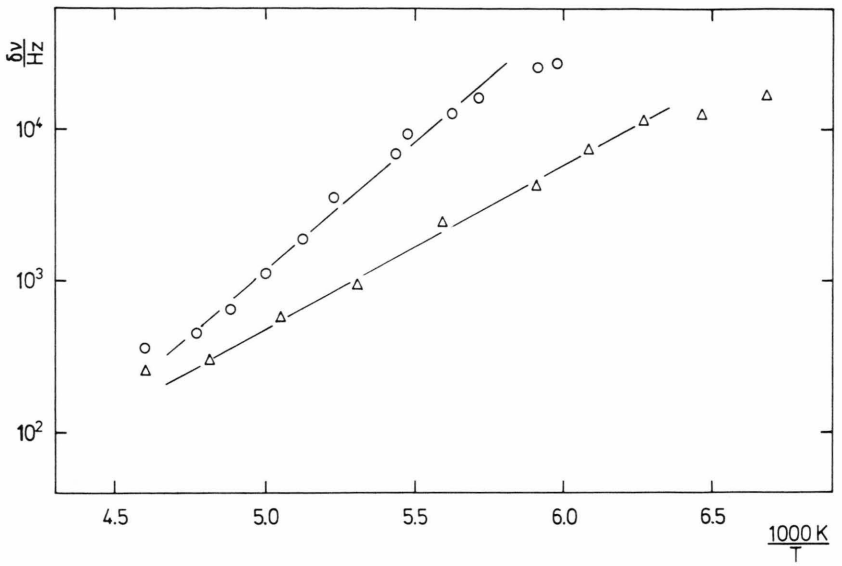

Fig. 3. Temperature dependence of the halfwidths of the ^{2}H NMR singlet lines of fluorobenzene on Graphon. (○) $\theta=1$; (△) $\theta=0.85$.

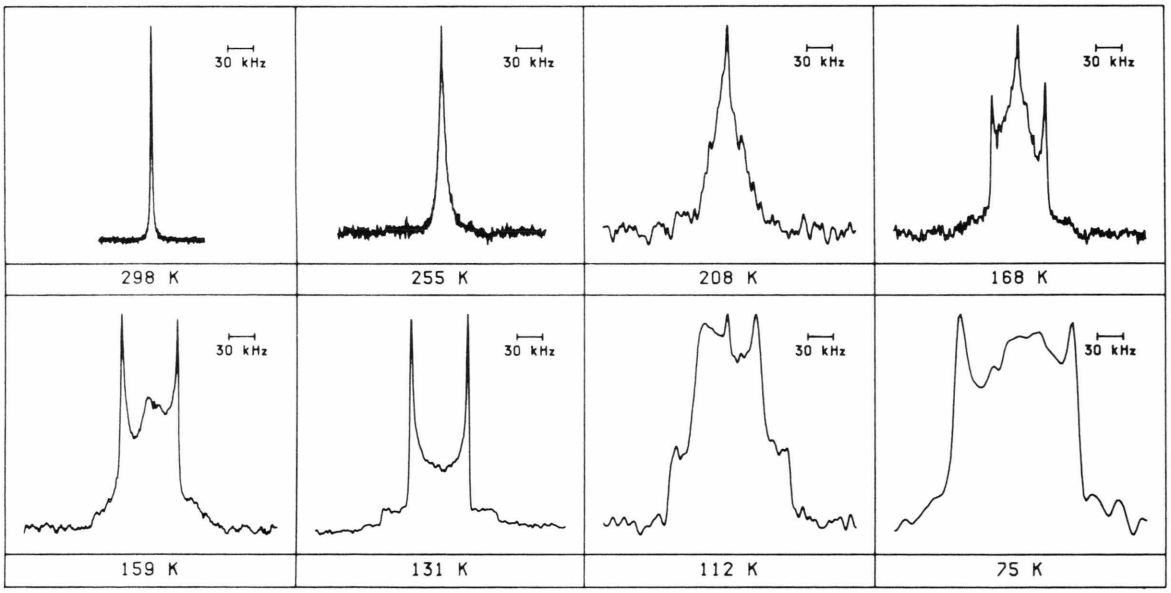

Fig. 4. ^{2}H NMR spectra of fluorobenzene adsorbed on boron nitride, $\theta=0.85$. In all cases the frequency axis runs from right to left.

IV. Discussion

1. Theoretical Basis for the Analysis of ^{2}H NMR Powder Patterns

In a high Zeeman field B_0 the NMR frequencies of a deuteron (^{2}H, spin $I=1$, electric quadrupole moment Q) which experiences both an electric quadrupole and a magnetic shielding coupling characterized by an axially symmetric electric field gradient (EFG) $\boldsymbol{q}$ and a magnetic shielding $\boldsymbol{S}$ tensor, respectively, may be formulated as

$$\left.\begin{matrix}\nu_{10}\\ \nu_{0-1}\end{matrix}\right\} = \nu_0 \mp \tfrac{1}{3}\nu_q(3\cos^2\theta_q - 1) - \tfrac{1}{3}\nu_S(3\cos^2\theta_S - 1). \quad (1)$$

Here the two resonance frequencies are labelled with the magnetic quantum numbers of the spin states be-

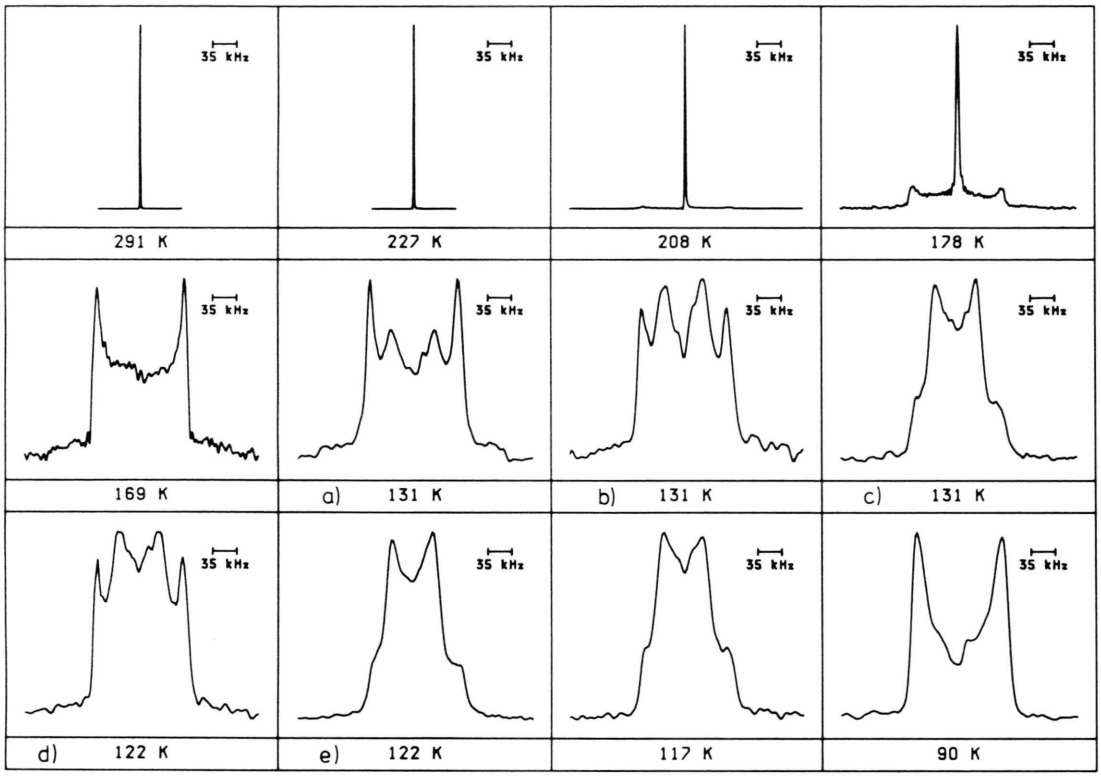

Fig. 5. ^{2}H NMR spectra of fluorobenzene adsorbed on Graphon, $\theta = 8$. The recycle delay times applied for the spectra at 131 and 122 K are (a) 1 s; (b) 0.25 s; (c) 0.1 s; (d) 0.75 s; (e) 0.1 s. In all cases the frequency axis runs from right to left.

tween which the resonant transitions occur. In (1)

$$\begin{aligned} \nu_0 &= \nu_Z(1-s_0) \equiv (\gamma/2\pi)\, B_0(1-s_0)\,, \\ \nu_q &= \tfrac{9}{8}\,\mathrm{DQCC}, \\ \nu_S &= \nu_Z\, \Delta s, \end{aligned} \tag{2}$$

where ν_Z is the Zeeman frequency, γ the gyromagnetic ratio, DQCC the deuteron quadrupole coupling constant, s_0 the isotropic shielding constant and Δs the shielding anisotropy. θ_q and θ_s are the angles between the Zeeman field and the distinct principal axes of the tensors $\boldsymbol{q}$ and $\boldsymbol{S}$, respectively.

For random orientation of the tensors $\boldsymbol{q}$ and $\boldsymbol{S}$ under the constraint of constant angle β between them, the NMR subpatterns corresponding to the single angle orientation frequencies ν_{10} and ν_{0-1} of (1) have been calculated [4]. These subpatterns may be characterized by the principal axis frequencies $\nu_{10}(J)$ and $\nu_{0-1}(J)$ $(J = X, Y, Z)$ of composite tensors $\boldsymbol{\nu}_{10}$ and $\boldsymbol{\nu}_{0-1}$ which, in general, unlike their constituents $\boldsymbol{q}$ and $\boldsymbol{S}$ are no longer axially symmetric. The principal axis frequencies depend parametrically on the angle β defined above, and on

$$A = \frac{\nu_s}{\nu_q} \equiv \frac{8}{9}\,\frac{\nu_Z\, \Delta s}{\mathrm{DQCC}}\,, \tag{3}$$

which is the ratio of the coupling strengths of the tensors $\boldsymbol{q}$ and $\boldsymbol{S}$ (see (1) and (2)). In the realm of this formalism $\nu_0 = (1/3)\,\mathrm{Tr}\{\boldsymbol{\nu}_{10}\} = (1/3)\,\mathrm{Tr}\{\boldsymbol{\nu}_{0-1}\}$.

Figure 6 a–c shows calculated powder patterns for cases which are of importance in the following discussion.

a) $A = 0$, i.e. the pure quadrupole case. Here, by superposition of the subpatterns ν_{10} and ν_{0-1}, which are mirror images of each other with respect to the central frequency $\nu_0 = \nu_Z$, the well known Pake type pattern is obtained. From the splitting $\Delta\nu$ of the distinct edges the quadrupole coupling constant is obtained as

$$\mathrm{DQCC} = (4/3)\, \Delta\nu\,. \tag{4}$$

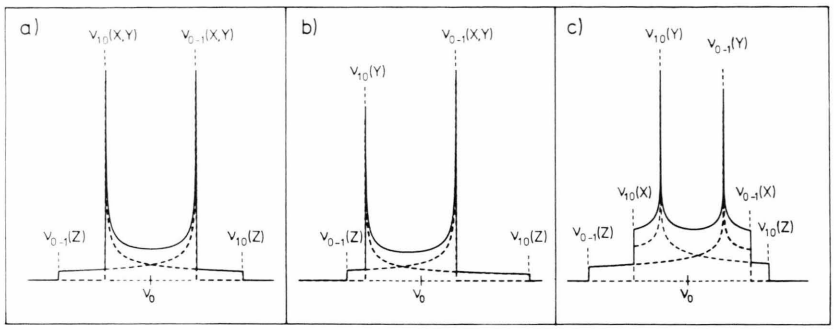

Fig. 6. Calculated spin $I=1$ patterns in the case of combined electric quadrupole and magnetic shielding coupling.
(a) $A=0$; (b) $A=0.2$, $\beta=0°$;
(c) $A=0.2$, $\beta=90°$.

b) $0<A\leqq 1$, $\beta=0°$. Using (16) and (23) of [4]:

$$\nu_{10}(X)=\nu_{10}(Y)=\nu_0+\tfrac{3}{8}\,\mathrm{DQCC}(1+A),$$
$$\nu_{10}(Z)\qquad\quad=\nu_0-\tfrac{3}{4}\,\mathrm{DQCC}(1+A), \tag{5}$$

and

$$\nu_{0-1}(X)=\nu_{0-1}(Y)=\nu_0-\tfrac{3}{8}\,\mathrm{DQCC}(1-A),$$
$$\nu_{0-1}(Z)\qquad\quad=\nu_0+\tfrac{3}{4}\,\mathrm{DQCC}(1-A). \tag{6}$$

Combination of (5) and (6) gives, after some rearrangement,

$$\mathrm{DQCC}=(4/3)(\nu_{10}(X)-\nu_{0-1}(Y)),$$
$$A=\frac{\nu_{10}(X)+\nu_{0-1}(Y)-2\nu_0}{\nu_{10}(X)-\nu_{0-1}(Y)}. \tag{7}$$

In contrast to case a), the typical edges are asymmetrically displaced with respect to ν_0. Most characteristically, in comparison to the symmetric case a) the outer side edges are displaced to lower frequency with respect to ν_0 whereas for the main edges the reverse displacement holds true. This leads to the typical asymmetric extension of the "feet" with the longer extended foot on the low frequency side.

c) $0<A\leqq 1$; $\beta=90°$. Here the distinct principal axes of $\boldsymbol{q}$ and $\boldsymbol{S}$ are perpendicular to each other. The following relations are obtained:

$$\nu_{10}(X)=\nu_0+\tfrac{3}{8}\,\mathrm{DQCC}(1+A),$$
$$\nu_{10}(Y)=\nu_0+\tfrac{3}{8}\,\mathrm{DQCC}(1-2A),$$
$$\nu_{10}(Z)=\nu_0-\tfrac{3}{4}\,\mathrm{DQCC}(1-\tfrac{1}{2}A), \tag{8}$$

and

$$\nu_{0-1}(X)=\nu_0-\tfrac{3}{8}\,\mathrm{DQCC}(1-2A),$$
$$\nu_{0-1}(Y)=\nu_0-\tfrac{3}{8}\,\mathrm{DQCC}(1-A),$$
$$\nu_{0-1}(Z)=\nu_0+\tfrac{3}{4}\,\mathrm{DQCC}(1+\tfrac{1}{2}A). \tag{9}$$

The rearrangement of these equations yields the same expressions for DQCC and A as in (7). In comparison to case a), the characteristics of the pattern here are the lifting of the X and Y degeneracies, the displacement of the outer side edges to higher frequency, and the divergent displacements of the outer main edges such that the less extended "foot" appears on the low frequency side of the pattern.

2. Fluorobenzene on Graphon, $\theta=1$ and $\theta=0.85$

In this section the foregoing theoretical considerations are applied to the deuterons in fluorobenzene adsorbed on the exposed basal planes of the graphite microcrystallites of Graphon. Here $\boldsymbol{q}$ is the intramolecular rigid or rotationally averaged EFG tensor in the cases where on the time scale $\tau_{\mathrm{NMR}}=\nu_q^{-1}$ (microsecond range) the spin carrying molecules retain their orientation in space and execute rapid reorientations around a spaced fixed axis, respectively. In the former case the main principal tensor component q is in line with the carbon/hydrogen bond direction and $\mathrm{DQCC}=e^2qQ/h$, whereas in the latter case q lies along the axis of rotation and [12]

$$\mathrm{DQCC}=\tfrac{1}{2}\,|\,3\cos^2\Delta-1\,|\,\frac{e^2qQ}{h}, \tag{10}$$

where Δ is the angle between the C–D bond direction and the rotation axis. The magnetic shielding tensor $\boldsymbol{S}$ is extramolecular in origin and is due to the polarization of the graphite support in the strong Zeeman field B_0 applied [1]. For symmetry reasons, the distinct principal axis of $\boldsymbol{S}$ is parallel to the normal of the exposed basal plane patch on which the deuteron carrying molecules are adsorbed [1].

The experimental powder patterns in the 130–110 K region (Fig. 2) exhibit the same type of asymmetry as the theoretical spectrum of Fig. 6 b, indicating that the

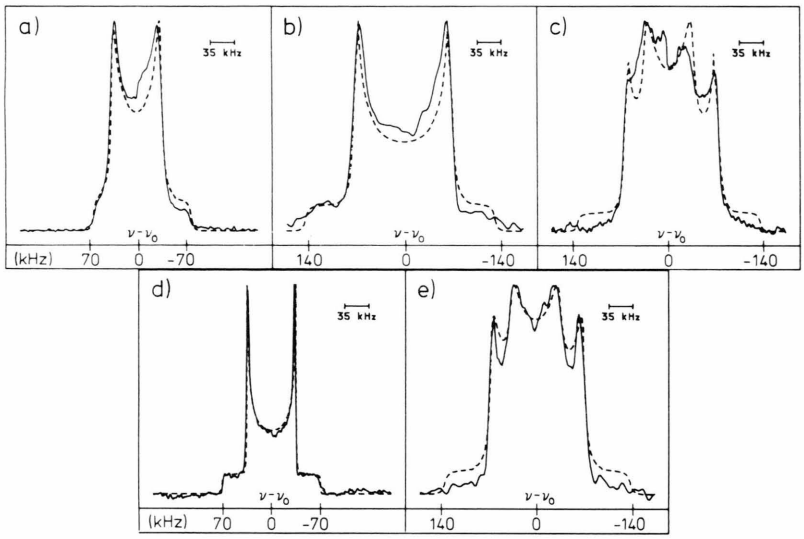

Fig. 7. Comparison of experimental and fitted powder patterns of fluorobenzene on Graphon (G) and on boron nitride (BN). The fit parameters are collected in Table 1. a) G, $\theta=1$, 131 K; b) G, $\theta=1$, 75 K; c) G, $\theta=1$, 90 K; d) BN, $\theta=0.85$, 131 K; e) G, $\theta=8$, 122 K; recycle delay time 0.75 s.

Table 1. Parameter values obtained from the fitting of ^{2}H NMR patterns.

Pattern in Fig. 7	DQCC/kHz	β	A	Δs/ppm	$\delta\nu$/kHz
a)	96 ± 2	0°	0.0732	150	6
b)	186 ± 3	90°	0.0378	150	7
c)	96 ± 5	0°	0.0732	150	12
	182 ± 3	90°	0.0386	150	6
d)	96 ± 1	–	0	–	1
e)	96 ± 3	0°	0.0732	150	13
	184 ± 3	–	0	–	8

distinct principal axes of $\boldsymbol{q}$ and $\boldsymbol{S}$ are parallel to each other ($\beta=0$). The parameters A and DQCC may be obtained from the characteristic edge frequencies using (5)–(6) or, more accurately, from a fitting of the spectrum shape which takes into account the individual line broadening $\delta\nu$. Figure 7a shows the fit which reproduces very well the pattern at 131 K. The parameter data used are collected in Table 1. The values of $\delta\nu$ (Lorentzian line shape) as well as of the shielding anisotropy Δs from A using (3) are in good agreement with the corresponding data obtained with benzene [1] and several methylaromatics [5] as the adsorbates. ν_0 was determined to be $52{,}720 \pm 1$ kHz.

The value obtained for DQCC is one half of the rigid coupling constant e^2qQ/h of deuterium attached to aromatic rings (180–190 kHz, [12–14]). The rotational averaging behind is the rapid rotation around the normal to the molecular plane, since $\Delta=90°$ put into (10) just yields this result. This implies that the distinct principal axis of $\boldsymbol{q}$ is along this normal and therefore is parallel to the normal to the surface since $\beta=0$. So, clearcut evidence is obtained that at the temperature in the range 130 to 110 K the molecules are adsorbed flat on the surface while being in a state of rapid planar rotation.

At the temperature 75 K the edge splitting is about twice the corresponding value in the range 130–110 K, i.e. DQCC is the rigid coupling constant e^2qQ/h. Here the planar rotation of the molecules is frozen in. Because of the efficient suppression of the "feet" it is not possible to decide unequivocally whether the well developed main edges are displaced asymmetrically about ν_0 or not. In this situation it is assumed that ν_0 at 75 K is practically the same as in the 130 to 110 K temperature region. As far as present knowledge goes, this assumption seems to be justified because at the temperatures under consideration the isotropic shielding constant s_0, which could account for a temperature dependence of ν_0, increases much more slowly with $1/T$ than at $T>130$, where $\Delta s_0/\Delta(1/T)$ is about 1.5 ppm/10^{-3} K^{-1} [15]. With this assumption, the distances of the edges from ν_0 are found to be different by about 5 kHz, where the larger distance is on the low frequency side. This type of asymmetry is typical for case c) discussed before with $\boldsymbol{q}$ and $\boldsymbol{S}$ having their distinct principal axes perpendicular to each other, i.e. the molecular C–D bond axes are in the surface plane. The calculated powder pattern is seen (Fig. 7b) to reproduce very well the experimental result. The parameters DQCC, Δs, and $\delta\nu$ applied in the calcula-

tion are collected in Table 1. The value of DQCC is in the expected range of e^2qQ/h, and Δs agrees nicely with the value derived from the previous patterns. These results give evidence that the molecules also in the rotationally frozen-in state are adsorbed flat on the surface.

The pattern determined at 90 K (Fig. 2a) is interpreted as the superposition of two separate patterns of the types observed at the lower and higher temperatures. Characteristically, the two superimposed patterns appear to be considerably shifted relative to each other. The calculated pattern with 45% and 55% deuterons in rapidly and non-rotating molecules in flat orientation, respectively, is obviously in nice agreement with experiment (Figure 7c).

From the NMR point of view the transformation of the solid state pattern into the singlet shape which is observed at temperatures >130 K is due to the rapid isotropic averaging of both the quadrupolar and the shielding type nuclear spin interaction. The averaging of $\boldsymbol{q}$ requires an isotropic reorientation of the molecular axis of planar rotation. This can be accomplished either by an in-place molecular reorientation or by surface diffusion across the outer surface of the adsorbent particles [16] even if the molecules retain their flat orientation. The averaging of $\boldsymbol{S}$, on the other hand, requires the latter mechanism to be operative. Here the rotation of $\boldsymbol{S}$ is the consequence of the place exchange of the molecules among the surface patches of different spatial orientation. So, the observed isotropic averaging must be due to the dynamic process of surface diffusion.

A rough estimate of the surface diffusion constant D can be obtained from the singlet linewidths $\delta\nu$ (Fig. 3) as follows. If the Graphon particles are considered as spheres of radius a, the surface diffusion of the molecules is obtained according to the relations [16, 17]

$$\delta\nu = \frac{9\pi}{20}\,(\mathrm{DQCC})^2\,\tau_M \tag{11}$$

and

$$D = \frac{a^2}{6\tau_M}. \tag{12}$$

In these equations τ_M is the correlation time of isotropic rotation. The linearity of the Arrhenius type $\delta\nu$ vs. $1/T$ plots (Fig. 3) suggests to write the correlation time as $\tau_M = \tau_{M_0}\exp(E/RT)$ where E is the activation energy of the surface diffusion process. The straight-forward analysis of the experimental linewidth data using (11) and (12) with $a=20$ nm [19] and DQCC $=93$ kHz from the 131 K solid state patterns yields $D/\mathrm{m^2\,s^{-1}} = 0.1\cdot\exp(-34\ \mathrm{kJ\ mol^{-1}}/RT)$ and $5\cdot10^{-3}\cdot\exp(-23\ \mathrm{kJ\ mol^{-1}}/RT)$ at the surface coverages $\theta=1.0$ and 0.85, respectively. At 200 K and $\theta=1$ the diffusion constant comes out as $D(200\ \mathrm{K}) = 1\cdot10^{-10}\ \mathrm{m^2\,s^{-1}}$, which compares well with the value for benzene adsorbed on Graphon [3].

In the discussion carried through so far the question was left open about the nature of the molecular processes that cause the shape transitions in the temperature regions 150–130 K and around 90 K. The first of these transitions might be explained as a dynamic effect if a broad distribution of the correlation times τ_M is prevailing so that either the rapid ($\tau_M \ll \tau_{NMR}$) or the slow ($\tau_M \gg \tau_{NMR}$) exchange cases are realized for the majority of the resonant spins. Since $\tau_M \propto a^2$ according to (12), such a distribution should result from the distribution of the particle sizes d. However, the latter distribution is so narrow (Fig. 8) that with 95% probability d^2 spans a range where the values of τ_M are different by less than the factor 5. So, an interpretation of the results in terms of the dynamic line shape analysis seems highly improbable. Therefore, the type of line shape change observed is explained to be due to a two-dimensional (2D) fluid-solid phase transition with a concomitant jump of τ_M through the NMR time scale τ_{NMR}. The observed gradual character of the transition is conceivable to be due to the circumstance that in contrast to a 2D first order constant pressure solidification the chemical potential of at least the fluid phase depending on its surface concentration

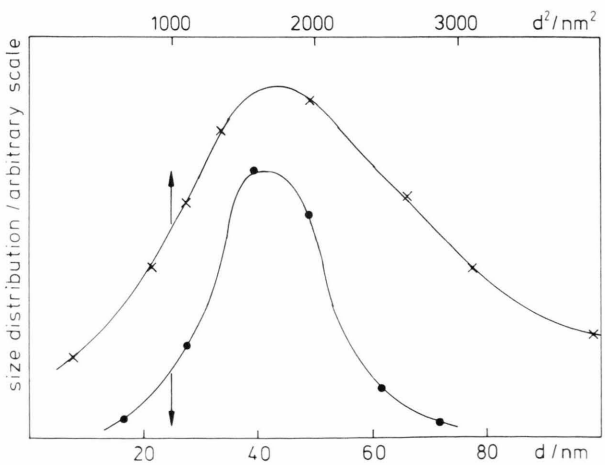

Fig. 8. Distribution of the Graphon particle sizes d and of d^2 (after Neue [8]).

does not remain constant when the partition of matter between the two phases in equilibrium with each other is changed by the phase transformation. The shift to lower temperature of the shape transition region of the $\theta = 0.85$ in comparison to the $\theta = 1$ sample is in accordance with this interpretation because the smaller surface concentration implies a lower chemical potential of the fluid phase.

The 2D solid phase formed in the transformation just considered is rotationally disordered as is evidenced by the ^{2}H NMR results. Probably, the transition of the spectrum shape and width below 100 K corresponds to a 2D solid-solid phase transformation into a rotationally ordered phase. This notion cannot be proved on the basis of the NMR results but requires diffraction techniques to be applied.

It is interesting to compare the behaviour of the fluorobenzene and benzene monolayers on the surface of Graphon. In the latter case [3] the 2D-fluid-solid phase transition takes place at a ca. 30 K lower temperature. The 2D solid phase is ordered [20], where the molecules lie flat on the surface and reorient rapidly around their hexad symmetry axis [1]. This state of rapid molecular reorientation persists even at temperatures as low as 75 K. The diverging behaviour of fluorobenzene is most reasonably attributed to the action of the dipole forces which cause the 2D fluid-solid transition to occur at higher temperature and the 2D solid-solid phase transition to come into existence.

3. Fluorobenzene on Boron Nitride, $\theta = 0.85$

The spectra of this system (Fig. 4) may be interpreted in a similar way as those of fluorobenzene on Graphon discussed in the previous section. Therefore, the discussion to follow concentrates on the major differences which have their origin in the different morphology and diamagnetic properties of the adorbents under consideration. In comparison to graphite both the trace and the anisotropy of the diamagnetic susceptibility tensor of boron nitride are lower by a factor of about 1000 [1], so that the extramolecular shielding effects can be neglected in comparison to the electric quadrupole coupling.

Assuming the surface diffusion coefficient of fluorobenzene to be of similar magnitude on both boron nitride and Graphon, the greater widths of the singlets for the former adsorbent can easily be attributed to its larger mean particle diameter, which conclusion is readily inferred from (11) and (12). Since the distribution of the particle sizes d comprises about two (section II), and therefore d^2 about four orders of magnitude, the line shape transitions between about 210 and 160 K (Fig. 4) can, at least in part, be characterized as a dynamical line shape transition, which mechanism in the previous section was concluded not to be responsible for the line shape transition observed for Graphon. At the temperature 168 K, for instance, the Pake type pattern spectrum component exhibiting the sharp edges at 70 kHz separation, may be considered to come from molecules which are confined to the plane surface of the large diameter platelets for times larger than the NMR time scale, whereas the central portion reflects the signals from molecules on smaller particles where the averaging of the quadrupole energy through surface diffusion takes place. A 2D fluid-solid transition as in the case of fluorobenzene on Graphon may interfere but cannot be identified.

The absence of the magnetic shielding coupling is demonstrated by the symmetric appearance of the pattern at 131 K (Figure 4). In fact, the agreement of experiment and fit (Fig. 7d and Table 1) based on the case a) assumption, is excellent. Actually, the molecules reorient rapidly about the axis normal to the molecular plane as on Graphon. This suggests the lying flat orientation which, however, cannot be proved in this case. Due to the sharply developed contours of the pattern at 131 K corresponding to a low value of the individual line width $\delta\nu$ (Table 1), the rigid deuteron quadrupole coupling constant in fluorobenzene is determined as $e^2qQ/h = 186 \pm 3$ kHz, which value has not been reported before in the literature.

4. Fluorobenzene on Graphon, $\theta = 8$

The narrow singlets and the Pake type quadrupole patterns which show up in the 290–190 K temperature range, are attributed to molecules in the adsorbed liquid like and the bulk (3D) solid phase, respectively. The latter is considered to consist of microcrystallites residing anywhere in the closed sample container.This phase is formed first when at some temperature well below the bulk melting point (−41.2 °C) the chemical potentials of the adsorbed and the bulk phases become equal. With further decreasing temperature equilibrium is maintained through successive desorption by which the coverage dependent chemical potential is properly adjusted. This process may cease if at

some surface coverage the enthalpy of desorption rises beyond the enthalpy of sublimation. This situation is prevailing at about monolayer coverage, which notion will be substantiated in the following.

The interpretation of the spectra at 131 and 122 K (Fig. 5) is straightforward. The narrower component which survives at short recycle delay times (τ_{rd}) must be attributed to molecules in close contact with the graphite surface, whereas the broad component represents the 3D solid phase. The agreement of the short recycle delay pattern and the spectra obtained at surface coverages $\theta = 0.85$ and 1 suggests that here the 2D and 3D solid phases coexist in equilibrium with each other.

The correctness of this assignment may be verified by comparing the experimental two-component spectra (Fig. 5) with calculated patterns. For the 3D solid, $\nu_0 = \nu_Z$ and the prominent edges are symmetrically displaced about ν_Z whereas for the adsorbed fluorobenzene, $\nu_0 = \nu_Z(1 - s_0)$ and an asymmetric displacement of the edges is prevailing. At 120 K the isotropic shift of deuterons on graphite is about -20 ppm relative to TMS [15] and therefore about -30 ppm relative to fluorobenzene since the hydrogen resonances of aromatics are about 5–10 ppm downfield from TMS. This implies an about 30 ppm or 1.5 kHz displacement to lower frequency of ν_0 for the adsorbed phase in comparison to the 3D solid. Taking this circumstance into account, the pattern calculated by superposition of an asymmetric subpattern with the data obtained for the one monolayer sample (Fig. 7a) and of a symmetric subpattern with DQCC = 186 kHz, reproduces excellently the experimental spectrum at 122 K ($\tau_{rd} = 750$ ms), as is shown in Figure 7e.

Acknowledgements

Financial support of this work by Deutsche Forschungsgemeinschaft und Fonds der Chemischen Industrie is gratefully acknowledged.

[1] B. Boddenberg and R. Grosse, Z. Naturforsch. **41a,** 1361 (1986).
[2] B. Boddenberg, in: Lectures on Surface Science (G. R. Castro and M. Cardona, eds.), Springer, Berlin 1987, p. 226.
[3] R. Grosse and B. Boddenberg, Z. Phys. Chem. NF **152,** 1 (1987).
[4] B. Boddenberg and G. Neue, Z. Naturforsch. **42a,** 948 (1987).
[5] B. Boddenberg and R. Grosse, Z. Naturforsch, **43a,** 497 (1988).
[6] B. Boddenberg and R. Grosse, Z. Naturforsch. **42a,** 272 (1987).
[7] Handbook of Chmistry and Physics (R. C. Weast, ed.), CRC Press, Boca Raton, 67th ed., 1986/87.
[8] G. Neue, Habilitationsschrift, Dortmund Univ. 1988
[9] B. K. Sahay and M. J. D. Low, J. Coll. Interf. Sci. **48,** 20 (1974).
[10] J. H. Davis, K. R. Jeffrey, M. Bloom, M. I. Valic, and T. P. Higgs, Chem. Phys. Letters **42,** 390 (1976).
[11] M. Rinne and J. Depireux, in: Advances in Nuclear Quadrupole Resonance (I. A. S. Smith, ed.), Heyden, London 1974, Vol. 74, p. 357.
[12] R. G. Barnes, in: Advances in Nuclear Quadrupole Resonance (J. A. S. Smith, ed.), Heyden, London 1974, Vol. 1, p. 335.
[13] H. H. Mantsch, H. Saito, and I. C. P. Smith, Progr. NMR Spectrosc. **11,** 211 (1977).
[14] C. Brevard and J. P. Kintzinger, in: NMR and the Periodic Table (R. K. Harris and B. E. Mann, eds.), Acad. Press, New York 1978, p. 107–128.
[15] G. Neue, Ph.D. Thesis, Univ. Dortmund 1983.
[16] B. Boddenberg and B. Beerwerth, J. Phys. Chem. **93,** 1440 (1989).
[17] R. Burmeister, H. Schwarz, and B. Boddenberg, Ber. Bunsenges. Phys. Chem. **93,** 1309 (1989).
[18] A. Abragam, The Principles of Nuclear Magnetism, Clarendon, Oxford 1961.
[19] G. Neue and B. Boddenberg, Molec. Phys. **68,** 771 (1989).
[20] U. Bardi, S. Magnanelli, and G. Rovida, Surf. Sci. **165,** L7 (1986).